
Deep learning and MCMC with aggVAE for shifting administrative boundaries: mapping malaria prevalence in Kenya

Elizaveta Semenova¹

Swapnil Mishra²

Samir Bhatt³

Seth Flaxman¹

H Juliette T Unwin⁴

¹Department of Computer Science, University of Oxford

²Saw Swee Hock School of Public Health and Institute of Data Science, National University of Singapore and NUHS

³School of Public Health, University of Copenhagen; School of Public Health, Imperial College London

⁴School of Public Health, Imperial College London; Department of Mathematics, University of Bristol

Abstract

Model-based disease mapping remains a fundamental policy-informing tool in public health and disease surveillance. Hierarchical Bayesian models have become the state-of-the-art approach for disease mapping since they are able to capture structure in the data, as well as to characterise uncertainty. When working with areal data, e.g. aggregates at the administrative unit level such as district or province, routinely used models rely on the adjacency structure of areal units to account for spatial correlations. The goal of disease surveillance systems is to track disease outcomes over time. This task provides challenging in situations of crises, such as political changes, leading to changes of administrative boundaries. Kenya is an example of a country where change of boundaries took place in 2010. Moreover, the adjacency-based approach ignores the continuous nature of spatial processes and cannot solve the change-of-support problem, i.e. when administrative boundaries change or when estimates must be produced at a different administrative level. We present a novel, practical, and easy to implement solution relying on a methodology combining deep generative modelling and fully Bayesian inference: we build on the recently proposed PriorVAE method able to encode spatial priors over small areas with variational autoencoders, to map malaria prevalence in Kenya. Our contributions can be summarised as follows:

- We view spatial process as continuous, instead of adjacency-based, and draw Gaussian Process (GP) realisations over an artificially created fine grid covering the domain of interest.
- We aggregate GP realisation separately over old and new administrative boundaries to obtain unit-specific random effects. We use the recently proposed PriorVAE technique to jointly encode GP aggregates over old and new administrative boundaries with variational autoencoders.
- The trained prior, termed *aggVAE*, is used within

Markov chain Monte Carlo (MCMC) inference scheme.

- We demonstrate that inference is orders of magnitude faster when using *aggVAE* prior than combining the original GP priors and the aggregation step.

1 INTRODUCTION

Malaria is still one of the major causes of mortality in sub-Saharan Africa, with a disproportionate burden on young children. In Kenya, a country with a long history of malaria control, approximately 75% of the population was still at risk in 2022 [U.S. President’s Malaria Initiative, 2022]. As malaria control programs continue to create novel control strategies, district-level disease mapping remains a fundamental surveillance tool for analysing the present and historical distribution of the disease in both space and time. However, disease tracking becomes incredibly difficult in the situation of crises. For example, political factors have been historically driving decentralisation across developing countries often leading to changes in administrative boundaries. Many of countries have increased their number of sub-national administrative units, including more than twenty countries in sub-Saharan Africa [Hassan, 2016]. Some countries have experienced a few changes of boundaries, such as Kenya. From a methodological viewpoint, district-level disease mapping in Kenya can be challenging because administrative boundaries changed in 2010: while the old system consisted of 8 provinces and 69 districts (Figure 1, left), the new system contains 47 districts (Figure 1, middle) which do not coincide with the old boundaries. This change is hard to tackle with standard disease mapping tools.

Hierarchical Bayesian models are the state-of-the-art approach for disease mapping [MacNab, 2022, Kang et al., 2016, Wakefield et al., 2000] since they are able to capture structure in the data, as well as to characterise uncertainty. Modern literature builds on a series of the seminal works of Besag [1974], Clayton [1992], Bernardinelli and Montomoli [1992], Bernardinelli et al. [1997], Clayton et al. [1993]

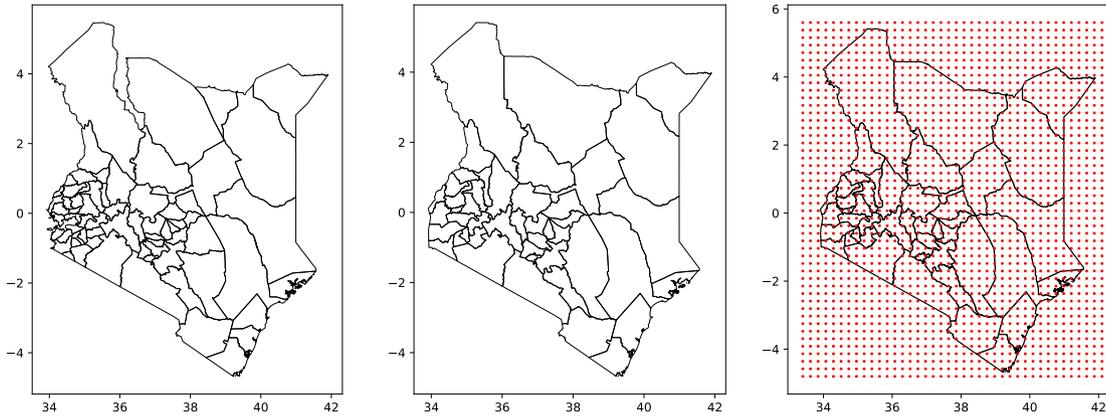


Figure 1: Map of Kenya with district borders before 2010 (left), district borders from 2010 (middle), and computational grid used (right).

which instigated a paradigm shift from the frequentist to Bayesian approach to disease mapping. The Bayesian disease mapping since the 1980s and 1990s has been used routinely with Bayesian hierarchical models as its foundation, with no shortage of examples in malaria mapping [Gemperli et al., 2006, Gosoni et al., 2006, Hay et al., 2009, Reid et al., 2010, Bhatt et al., 2015, 2017, Snow et al., 2017, Weiss et al., 2019]. It employed Markov chain Monte Carlo (MCMC) simulation methods for the Bayesian estimation, learning, and inference of unknown quantities and parameters. In recent years approximate inference algorithms, such as integrated nested Laplace approximation (INLA) have gained popularity [Martins et al., 2013]. While such tools provide extremely convenient interfaces to a set of predefined models, they do not provide enough flexibility for custom model development. They, hence, have limitations for specific classes of applied research. Simultaneous aggregation procedure and change-of-support which we tackle in this paper is one such example. MCMC, on the contrary, is a general sampling technique for sampling from a possibly unnormalised target density $\pi(z)$, i.e. the posterior [Robert et al., 1999, Gelman et al., 1995].

MCMC simulates an ergodic Markov chain $\{z^{(i)}\}_{i \in \mathbb{N}}$

that admits $\pi(z)$ as its unique limiting distribution. In practice, the simulation is performed for a finite number of iterations N , where N is sufficiently large for MCMC to converge. MCMC convergence and efficiency can be assessed via diagnostic tools, such as the \hat{R} statistic and effective sample size (ESS) metrics, correspondingly [Vehtari et al., 2021]. The \hat{R} statistic, also known as the potential scale reduction factor, is a measure used to assess the convergence of multiple MCMC chains by comparing the within-chain variance to the between-chain variance. The ESS statistic quantifies the amount of independent information obtained

from the generated samples, reflecting the effective size of the sample in terms of capturing the true underlying distribution. The main advantage of MCMCs is that they provide guarantees of producing asymptotically *exact* samples from the target density. In health policy-related applications where modelling informs decision making this property makes MCMC preferable to non-exact methods. While MCMC has proven to be very successful compared to simpler inference algorithms, it scales poorly for problems involving correlation structures, such as Gaussian Processes (GPs). Additional issues inherent to MCMC are auto-correlations of samples making sampling less efficient. It is highly desirable for disease mapping models to retain modelling flexibility and the ability to use MCMC, and, at the same time, to improve inference speed and efficiency.

The main modelling tool for capturing spatial correlation in a disease mapping model is GPs, whose realisation over a finite number of points is represented via a multivariate Normal (\mathcal{MVN}) distribution. The most common type of spatial data analysed in this context is the so called *areal* data, i.e., data obtained via aggregation of individual observations over spatial areas, such as administrative units. Statistical models describing areal data typically rely on the adjacency structure of areal units to account for spatial correlation. One drawback of this approach is that it disregards the continuous nature of underlying processes and potential heterogeneity within each region, especially large ones. Additionally, adjacency-based methods are very rigid with respect to the change-of-support problem, i.e., when administrative boundaries change or when mapping needs to be done at a different administrative level. The spatial aggregation process has been proposed in the literature to address this issue: an observational model is designed using the integration of the GP over the corresponding region

[Tanaka et al., 2019, Yousefi et al., 2019, Zhu et al., 2021, Johnson et al., 2019].

In this work, we present a novel, practical and easy to implement solution of the change-of-support problem relying on a methodology combining deep generative modelling and fully Bayesian inference. Our approach is twofold:

- We view the spatial process as continuous. Rather than performing modelling based on the adjacency structure, we model the latent GP process on a fine spatial scale over an artificial computational grid covering the domain of interest and obtain unit-level estimates via aggregation. This approach has been used before since it can better capture continuity than adjacency-based methods.
- We extend the recently proposed PriorVAE [Semenova et al., 2022] method of encoding spatial priors with variational autoencoders to the change-of-support problem and malaria prevalence mapping in Kenya. Realisations of GP priors are generated on a fine spatial grid, and then aggregated to the level of administrative units. The aggregated values are encoded using the PriorVAE technique. The trained priors, termed aggVAE, are then used at the MCMC inference stage instead of combining the generation of GP priors and the aggregation step at each MCMC iteration.

We show that the method using aggVAE priors is faster and more efficient within an MCMC inference scheme than the one relying directly on the GP priors.

The rest of this paper is structured as follows: in 2.1 we describe models from classical spatial statistics used to analyse areal data, in 2.2 we introduce the field of deep generative modelling and in particular the VAE architecture, in 2.3 we summarise the PriorVAE method of encoding spatial priors; then in 3 we propose the aggVAE method allowing to encode aggregated latent GP evaluations. Application to malaria prevalence mapping in Kenya is presented in 4 and we conclude by discussing limitations and future work in 5.

2 BACKGROUND

2.1 SPATIAL STATISTICS MODELS OF AREAL DATA

Classical statistical models describing areal data typically rely on the adjacency structure of areal units to account for spatial correlation. The prior on the spatial term in such models, in general, can be written as

$$f \sim \mathcal{MVN}(0, Q^{-1}),$$

where Q denotes the precision matrix. Adjacency characterises the neighborhood structure allowing to calculate Q based on the connectedness of the adjacent graph. These

methods take advantage of the tendency for neighboring areas to possess similar features. Besag [1974] first proposed the Conditional Auto-Regressive (CAR) with

$$Q = \tau(I - \alpha A),$$

where τ denotes the marginal precision, A is the adjacency matrix and α is a parameter capturing the amount of spatial dependence. Variations of this model were later proposed and include intrinsic CAR (iCAR) with [Besag et al., 1991]

$$Q = \tau(D - A),$$

where D is the diagonal matrix consisting of the total number of neighbours for each area, proper CAR (pCAR) [Cressie, 2015] with

$$Q = \tau(D - \alpha A),$$

Leroux CAR (LCAR) [Leroux et al., 2000] with

$$Q = \tau(\alpha(D - A) + (1 - \alpha)I),$$

Besag-York-Mollié (BYM) model [Besag et al., 1991] with

$$Q = \frac{1}{\tau_s}(D - A) + \frac{1}{\tau_{\text{id}}}I,$$

BYM2 [Riebler et al., 2016].

2.2 VARIATIONAL AUTOENCODERS (VAES)

A Variational Autoencoder (VAE) is a type of generative model that uses deep learning techniques to generate new data samples $\hat{y} \in \mathcal{Y} \subset \mathbb{R}^n$ that resemble the original training data $y \in \mathcal{Y}$. It consists of two parts: an encoder $E_\phi(\cdot)$ that maps input data to a lower-dimensional representation (latent space) $\mathcal{Z} \subset \mathbb{R}^d$, $d < n$, and a decoder $D_\psi(\cdot)$ that maps the latent representation $z \in \mathcal{Z}$ back to the original data space. The encoder and decoder are trained together to minimise a reconstruction loss, which measures the difference between the original data and its reconstructed version. Additionally, a constraint is imposed on the latent representation to follow a prior distribution $q(z|y)$, such as a Gaussian distribution, allowing the model to generate new, unseen data by sampling from the prior and passing it through the decoder. Following Kingma and Welling [2013], the optimal parameters for the encoder and decoder are found by maximising the evidence lower bound:

$$\mathcal{L}_{\text{VAE}} = \mathbb{E}_{q(z|y)} [\log p(y|z)] - KL[q(z|y)||p(z)].$$

The prior of the latent space and the variational distribution are typically chosen to have Gaussian forms: $p(z) = \mathcal{N}(0, I_d)$, $q(z|y) = (\mu_z, \sigma_z^2 I_d)$.

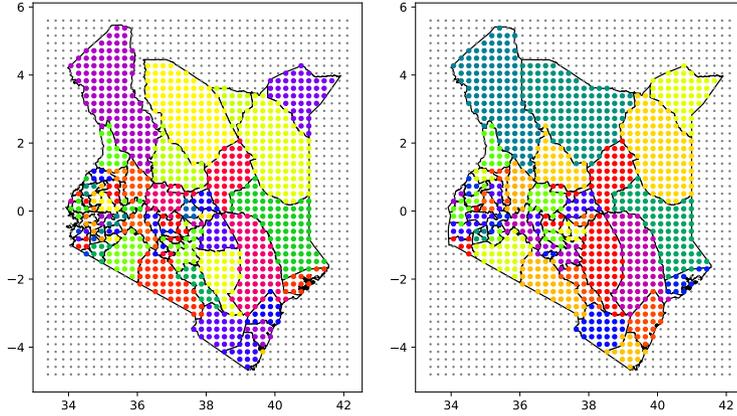


Figure 2: Attribution of grid points over polygons (districts) before 2010 in (left), and from 2010 in (right). Grey points correspond to points falling outside of the country’s borders, and points falling within the same polygon are represented with the same color.

2.3 ENCODING SPATIAL PRIORS WITH VAES

π VAE [Mishra et al., 2022] and PriorVAE [Semenova et al., 2022] are two related VAE-based methods that can respectively encode continuous stochastic processes and their finite realisations. They utilize a trained decoder to approximate computationally complex GPs and \mathcal{MVN} s for Bayesian inference with MCMC, preserving the rigor of MCMC while ensuring scalability through the simplicity of the VAE’s latent space. The key difference between the two methods is the type of prior they encode and the method of encoding: π VAE uses a low-dimensional embedding of function classes via a combination of a trainable feature mapping and a generative model, based on the Karhunen-Loeve Expansion concept, while PriorVAE directly encodes GP realisations. In this work we will follow the PriorVAE route. The method has been proposed as a scalable solution to the small area estimation (SAE) problem in spatial statistics as it encodes realisations of priors presented in 2.1. A characteristic property of PriorVAE is that it needs to be trained on a predefined spatial structure. On one hand, this is a disadvantage compared to π VAE since PriorVAE is unable to make predictions on off-grid locations. On the other hand, in the settings when the spatial structure is known in advance, PriorVAE is preferred due to its simpler computational setup, as only the prior-encoding VAE needs to be trained, without the need for learning of the feature map. The inference workflow using the PriorVAE method can be described as follows:

- Fix the spatial structure of interest $\{x_1, \dots, x_n\}$ - a set of administrative units, or an artificial computational grid.

- Draw evaluations of a GP prior $\mathcal{GP}(\cdot)$ over the spatial structure and use the vector of realisations

$$f_{\text{GP}} = (f(x_1), \dots, f(x_n))^T$$

as data for a VAE to encode.

- Perform Bayesian inference of the overarching model using MCMC, where f_{GP} is approximated in a drop-on manner using the trained decoder $D_\psi(\cdot)$:

$$f_{\text{GP}} \approx \hat{f}_{\text{GP}} = f_{\text{PriorVAE}} = D_\psi(z_d), \quad z_d \sim \mathcal{N}(0, I_d).$$

3 ENCODING AGGREGATES OF THE GAUSSIAN PROCESS PRIOR: AGGVAE

3.1 GP EVALUATIONS OVER A FINE SCALE GRID

We view the underlying process as continuous and approximate it by evaluating the GP on a fine spatial grid $G = \{g_1, \dots, g_n\}$ (Figure 1 (right)) covering the domain of interest. The grid is regular and has been chosen to ensure that at least one point of the grid g_j lies within each administrative unit p_i . GP prior realisations $f(\cdot)$ are drawn over the artificial grid G as a multivariate normal distribution with a covariance matrix following the RBF¹ kernel:

$$f = \begin{pmatrix} f_1 \\ \vdots \\ f_n \end{pmatrix} \sim \mathcal{MVN}(0, \Sigma), \quad \Sigma_{jk} = \sigma^2 \exp\left(-\frac{d_{jk}^2}{2l^2}\right)$$

¹Any kernel can be used. We use RBF only as an example.

where $f_j = f(g_j)$, $d_{jk} = \|g_j - g_k\|$ and σ^2, l are hyperparameters of the Gaussian Process. For the hyperparameters we used $l \sim \text{InvGamma}(3, 3)$ and $\sigma \sim \mathcal{N}^+(0.05)$ priors.

3.2 COMPUTING GP AGGREGATES OVER POLYGONS

As the next step, we aggregate GP evaluations to the district level. Each district is viewed as a polygon $p_i, i = 1, \dots, K$, and the computation takes the form

$$f_{\text{aggGP}}^{p_i} = \int_{p_i} f(s) ds \approx c \sum_{g_j \in p_i} f_j = c \bar{f}_{\text{aggGP}}^{p_i}. \quad (1)$$

Here $\bar{f}_{\text{aggGP}}^{p_i} = \sum_{g_j \in p_i} f_j$ and we have used the midpoint quadrature rule. The constant $c = \Delta x \Delta y$ with Δx and Δy being step sizes of the grid along the x and y axes, respectively. We can, therefore, construct a vector where each entry represents a spatial random effect at a district p_i :

$$f_{\text{aggGP}} = \begin{pmatrix} \bar{f}_{\text{aggGP}}^{p_1} \\ \vdots \\ \bar{f}_{\text{aggGP}}^{p_K} \end{pmatrix} \in \mathbb{R}^K. \quad (2)$$

In practice, we implement 1 via matrix multiplication. For this, we precompute matrix M consisting of K rows and n columns with binary entries M_{ji} , indicating whether point j lies within polygon i (see Figures 2):

$$M_{ji} = I_{\{g_j \in p_i\}}, \quad j = 1, \dots, K, \quad i = 1, \dots, n.$$

Hence, M serves as a lookup table, and if f is a vector of GP draws over the grid, the product Mf gives the vector of sums

$$\bar{f}_{\text{aggGP}} = Mf = \begin{pmatrix} \bar{f}_{\text{aggGP}}^{p_1} \\ \vdots \\ \bar{f}_{\text{aggGP}}^{p_K} \end{pmatrix}. \quad (3)$$

This procedure can be performed both with respect to the old and new boundaries to obtain vectors $f_{\text{aggGP}}^{\text{old}}$ and $f_{\text{aggGP}}^{\text{new}}$, respectively, using M^{old} and M^{new} precomputed matrices.

3.3 ENCODING GP AGGREGATES

In order to tackle the change-of-support problem, we encode $\bar{f}_{\text{aggGP}}^{\text{old}}$ and $\bar{f}_{\text{aggGP}}^{\text{new}}$ jointly. We construct a vector of dimension $K_1 + K_2$ of the form

$$\bar{f}_{\text{aggGP}}^{\text{joint}} = \begin{pmatrix} \bar{f}_{\text{aggGP}}^{p_1^{\text{old}}} \\ \vdots \\ \bar{f}_{\text{aggGP}}^{p_{K_1}^{\text{old}}} \\ \hline \bar{f}_{\text{aggGP}}^{p_1^{\text{new}}} \\ \vdots \\ \bar{f}_{\text{aggGP}}^{p_{K_2}^{\text{new}}} \end{pmatrix} = \begin{pmatrix} M^{\text{old}} f \\ M^{\text{new}} f \end{pmatrix} \in \mathbb{R}^{K_1 + K_2}.$$

and apply the PriorVAE method to $\bar{f}_{\text{aggGP}}^{\text{joint}}$, i.e. we encode GP aggregates jointly for old and new boundaries with a VAE using a lower-dimensional representation with independent standard Gaussian components z_1, \dots, z_d , $d < K_1 + K_2$, $z_i \sim N(0, 1)$. We denote the new prior of the area-level spatial effect as f_{aggVAE} . This one-step prior can be used at the inference stage instead of the two step procedure where first evaluation f_1, \dots, f_n need to be drawn and then aggregated to obtain f_{aggGP} . We summarise the encoding and MCMC inference procedure using aggVAE in Algorithm 1.

- Fix spatial structure of areal units as a collection of polygons $P = \{p_1, \dots, p_K\}$.
- Create an artificial computational grid of sufficient granularity $G = \{g_1, \dots, g_n\}$.
- Precompute the matrix of indicators M , $M_{ji} = I_{\{g_j \in p_i\}}$.
- Draw GP evaluations over G using a selected kernel $k(\cdot, \cdot): f = (f_1, \dots, f_n)^T$.
- Compute GP aggregates at the level of $P: f_{\text{aggGP}} = cMf$
- Train PriorVAE on f_{aggGP} (or \bar{f}_{aggGP}) draws to obtain f_{aggVAE} priors
- Use f_{aggVAE} at inference within MCMC.

Algorithm 1: Inference procedure using aggVAE

4 INFERENCE USING AGGVAE: MAPPING MALARIA PREVALENCE IN KENYA

Malaria prevalence is routinely mapped using disease surveillance data which was collected, for example, via the DHS programme. A number of survey clusters (households) are selected and individuals within a cluster get tested for the presence or absence of malaria parasite. Malaria prevalence can then be modelled as the probability of a positive test among all tests. In this work we use results of the survey conducted in 2015. In 2010 administrative boundaries in Kenya changed (1). We treat the 2015 data as static, i.e. we assume that the same data was collected once before 2010 and once after 2010 by overlaying it with old and new boundaries. District-specific malaria prevalence $\theta_i, i \in 1, \dots, K$ is inferred using the Binomial distribution

$$\begin{cases} n_i^{\text{pos}} & \sim \text{Bin}(n_i^{\text{tests}}, \theta_i), \\ \text{logit}(\theta_i) & = b_0 + f_{\text{aggGP}}^{p_i}. \end{cases} \quad (4)$$

where n_i^{tests} and n_i^{pos} are the number of total and positive RDT tests observed in district i , correspondingly. $f_{\text{aggGP}}^{p_i}$ in 4 is the two-step spatial prior requiring first the sampling of

the GP draws and the subsequent aggregation step. To avoid this procedure, we approximate $f_{\text{aggGP}}^{P_i}$ with $f_{\text{aggVAE}}^{P_i}$ and use the following model for inference:

$$\begin{cases} n_i^{\text{pos}} & \sim \text{Bin}(n_i^{\text{tests}}, \theta_i), \\ \text{logit}(\theta_i) & = b_0 + s f_{\text{aggVAE}}^{P_i}. \end{cases} \quad (5)$$

The additional parameter s is introduced here to account for us encoding \tilde{f}_{aggGP} rather than f_{aggGP} , as well as to prevent our VAEs from oversmoothing; the additional parameter can correct for that at the inference stage.

Our goal is to compare speed and efficiency in terms of effective sample sizes (ESS) of MCMC inference using models described in 4 and 5. Both inference models were implemented using the NumPyro probabilistic programming language [Phan et al., 2019, Bingham et al., 2019] and the encoding of aggVAE was performed using the JAX library [Bradbury et al., 2018]. We ran both MCMC inference models using 200 warm-up and 1000 posterior samples. Results of the comparison are presented in Table 1. The model using aggGP prior ran 10K times longer, and after 14h has not fully converged. After 1200 total iterations it has only achieved $\hat{R} = 1.4$. Traceplots and posterior distributions for the GP lengthscale and variance parameter are presented on Figures 3 and 4, correspondingly. When comparing spatial random effects (REs) corresponding to old and new boundaries, aggGP model particularly struggles with the old ones: maximum Gelman-Rubin statistic is $\hat{R} = 1.10$ for REs over the old boundaries, and $\hat{R} = 1.06$ for REs over the new boundaries. Graphical comparison of the crude estimates, i.e. observed crude prevalence ($\theta_{\text{crude}} = \frac{n_i^{\text{pos}}}{n_i^{\text{tests}}}$) and estimates obtained by the aggGP and aggVAE models are presented on Figures 5 and 6, correspondingly. Maps of crude prevalence estimates, estimates obtained by the aggGP and aggVAE models are presented on Figure 7 for boundaries before 2010 and on Figure 8 for boundaries from 2010.

5 DISCUSSION AND FUTURE WORK

In this work we have demonstrated the applicability of aggregated GP priors to represent spatial random effect instead of traditional adjacency-based models, and presented a scalable solution to the change-of-support problem by jointly encoding GP aggregates using the PriorVAE technique. Modelling on fine resolution scales is attractive since this approach allows us to capture continuity, but it is computationally cumbersome. By introducing the aggVAE prior, we alleviate the computational difficulties. Our results showed that inference using aggVAE priors is orders of magnitude faster and more efficient than inference performed using the GP priors; effective sample size per second is thousands times

²After this time aggGP model has not fully converged; e.g. the Gelman-Rubin statistic for the lengthscale parameter is $\hat{R} = 1.4$.

Table 1: Comparison of MCMC for models with f_{aggGP} and f_{aggVAE} spatial random effects (REs) using 200 warm-up and 1000 steps

Model (used prior)	aggGP RE	aggVAE RE
Elapsed time	14h ²	8s
Average ESS of the REs	129	231
ESS per minute	0.15	1732
Maximum \hat{R} of REs, boundaries before 2010	1.10	1.01
Maximum \hat{R} of REs, boundaries from 2010	1.07	1.01
Average ESS of the REs, boundaries from 2010	132	222
Average ESS of the REs, boundaries from 2010	125	245

higher when using aggVAE prior than combining the original GP priors and the aggregation step to obtain aggGP. Our work lays foundation for future extensions allowing to capture heterogeneity of continuous covariates X , such as environmental factors, at a fine spatial scale, by including them into the linear predictor of the model as the fixed effect term: $b_0 + X\beta + f$. We used the RBF kernel to model GP on the fine spatial scale. This kernel defines smooth and stationary GP draws. However, the presented methodology is kernel-agnostic, and any other kernel can be used instead, including non-stationary kernels. One drawback of the PriorVAE method is pertinent in the current work as well: aggVAE is not explicitly encoding hyperparameters of the GP, such as lengthscale, and, hence, is not able to infer them. Future extensions should focus on closing this gap, e.g. conditional variational autoencoders can be used instead to overcome this issue [Semenova et al., 2023]. Since aggVAE provides a prior that does not have a closed form solution but is rather obtained in an empirical way by training a neural work, theoretical properties of such priors and their influence on downstream inference should be studied in more detail. While modelling prevalence, we have taken the number of positive and negative tests at their face values. Sensitivity of the test, however, may play a role. We also treated survey locations as noise-free, while due to privacy they have 10 km precision. Both facts should be taken into account while performing modelling for real-life applications and constitute future work.

Data and Code Availability Data containing administrative boundaries of Kenya are publicly available: current

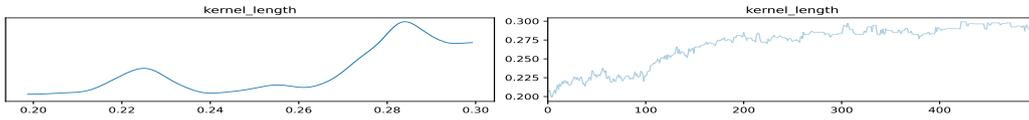


Figure 3: Posterior distribution (left) and traceplot (right) of the GP lengthscale parameter.

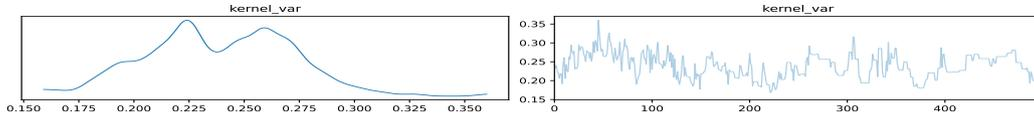


Figure 4: Posterior distribution (left) and traceplot (right) of the GP variance parameter.

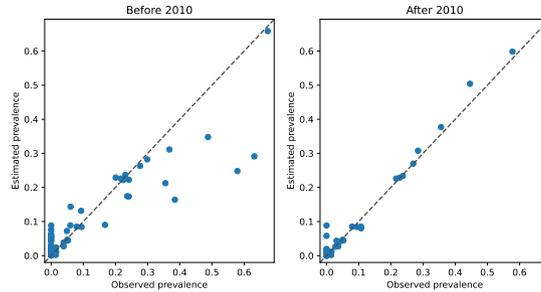


Figure 5: Observed and estimated prevalence produced by the aggGP model. The model has not converged after 1200 MCMC steps and particularly struggles with estimates over the old boundaries.

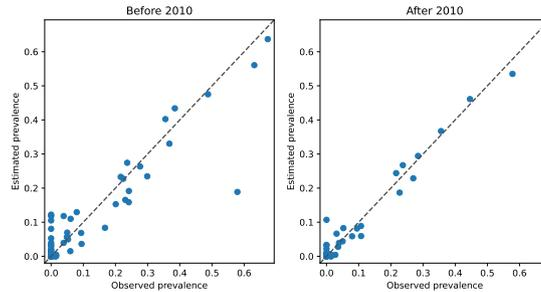


Figure 6: Observed and estimated prevalence produced by the aggVAE model.

boundaries³ and old boundaries⁴ can be freely downloaded. Malaria prevalence data was obtained from DHS 2015 survey and contains information on locations of clusters and test positivity to calculate district-specific prevalence; it can be requested from the DHS programme⁵. Code to reproduce the results is available at <https://github.com/MLGlobalHealth/aggVAE>.

³https://data.humdata.org/dataset/2c0b7571-4bef-4347-9b81-b2174c13f9ef/resource/03df9cbb-0b4f-4f22-9eb7-3cbd0157fd3d/download/ken_adm_iebc_20191031_shp.zip

⁴<https://www.wri.org/data/kenya-gis-data>

⁵<https://dhsprogram.com/>

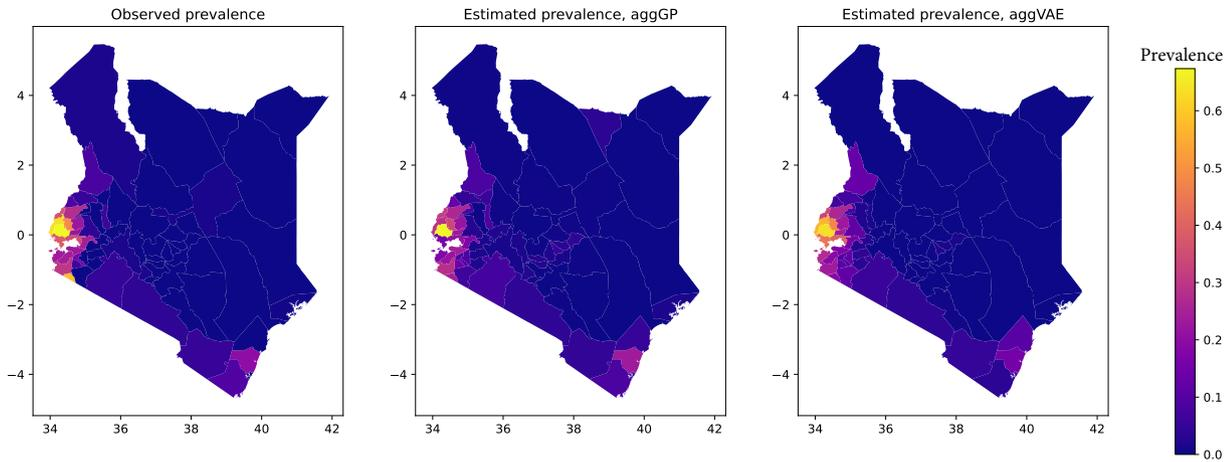


Figure 7: Map of malaria prevalence in Kenya based on district boundaries before 2010: (a) crude prevalence estimates, (b) estimates obtained by the aggGP model, and (c) estimates obtained by the aggVAE model.

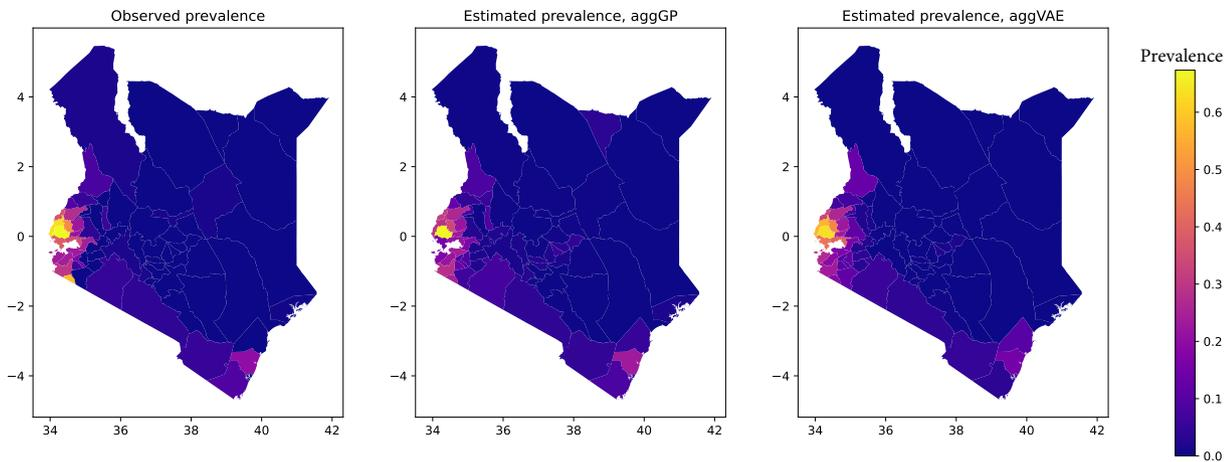


Figure 8: Map of malaria prevalence in Kenya based on district boundaries before 2010: (a) crude prevalence estimates, (b) estimates obtained by the aggGP model, and (c) estimates obtained by the aggVAE model.

References

- L Bernadinelli, Cristian Pascutto, NG Best, and WR Gilks. Disease mapping with errors in covariates. *Statistics in medicine*, 16(7):741–752, 1997.
- Luisa Bernardinelli and Cristina Montomoli. Empirical bayes versus fully bayesian analysis of geographical variation in disease risk. *Statistics in medicine*, 11(8):983–1007, 1992.
- Julian Besag. Spatial interaction and the statistical analysis of lattice systems. *Journal of the Royal Statistical Society: Series B (Methodological)*, 36(2):192–225, 1974.
- Julian Besag, Jeremy York, and Annie Mollié. Bayesian image restoration, with two applications in spatial statistics. *Annals of the institute of statistical mathematics*, 43:1–20, 1991.
- Samir Bhatt, DJ Weiss, E Cameron, D Bisanzio, B Mappin, U Dalrymple, KE Battle, CL Moyes, A Henry, PA Eckhoff, et al. The effect of malaria control on plasmodium falciparum in africa between 2000 and 2015. *Nature*, 526(7572):207–211, 2015.
- Samir Bhatt, Ewan Cameron, Seth R Flaxman, Daniel J Weiss, David L Smith, and Peter W Gething. Improved prediction accuracy for disease risk mapping using gaussian process stacked generalization. *Journal of The Royal Society Interface*, 14(134):20170520, 2017.
- Eli Bingham, Jonathan P. Chen, Martin Jankowiak, Fritz Obermeyer, Neeraj Pradhan, Theofanis Karaletsos, Rohit Singh, Paul A. Szerlip, Paul Horsfall, and Noah D. Goodman. Pyro: Deep universal probabilistic programming. *J. Mach. Learn. Res.*, 20:28:1–28:6, 2019. URL <http://jmlr.org/papers/v20/18-403.html>.
- James Bradbury, Roy Frostig, Peter Hawkins, Matthew James Johnson, Chris Leary, Dougal Maclaurin, George Necula, Adam Paszke, Jake VanderPlas, Skye Wanderman-Milne, and Qiao Zhang. JAX: composable transformations of Python+NumPy programs, 2018. URL <http://github.com/google/jax>.
- David G Clayton. Bayesian methods for mapping disease risk. *Geographical and environmental epidemiology: methods for small-area studies*, pages 205–220, 1992.
- David G Clayton, Luisa Bernardinelli, and Cristina Montomoli. Spatial correlation in ecological analysis. *International journal of epidemiology*, 22(6):1193–1202, 1993.
- Noel Cressie. *Statistics for spatial data*. John Wiley & Sons, 2015.
- Andrew Gelman, John B Carlin, Hal S Stern, and Donald B Rubin. *Bayesian data analysis*. Chapman and Hall/CRC, 1995.
- Armin Gemperli, Nafomon Sogoba, Etienne Fondjo, Musawenkosi Mabaso, Magaran Bagayoko, Olivier JT Briët, Dan Anderegg, Jens Liebe, Tom Smith, and Penelope Vounatsou. Mapping malaria transmission in west and central africa. *Tropical Medicine & International Health*, 11(7):1032–1046, 2006.
- Laura Gosoni, Penelope Vounatsou, Nafomon Sogoba, and Thomas Smith. Bayesian modelling of geostatistical malaria risk data. *Geospatial health*, 1(1):127–139, 2006.
- Mai Hassan. A state of change: district creation in kenya after the beginning of multi-party elections. *Political Research Quarterly*, 69(3):510–521, 2016.
- Simon I Hay, Carlos A Guerra, Peter W Gething, Anand P Patil, Andrew J Tatem, Abdisalan M Noor, Caroline W Kabaria, Bui H Manh, Iqbal R F Elyazar, Simon Brooker, et al. A world malaria map: Plasmodium falciparum endemicity in 2007. *PLoS medicine*, 6(3):e1000048, 2009.
- Olatunji Johnson, Peter Diggle, and Emanuele Giorgi. A spatially discrete approximation to log-gaussian cox processes for modelling aggregated disease count data. *Statistics in medicine*, 38(24):4871–4887, 2019.
- Su Yun Kang, Susanna M Cramb, Nicole M White, Stephen J Ball, and Kerrie L Mengersen. Making the most of spatial information in health: a tutorial in bayesian disease mapping for areal data. *Geospatial health*, 11(2), 2016.
- Diederik P Kingma and Max Welling. Auto-encoding variational bayes. *arXiv preprint arXiv:1312.6114*, 2013.
- Brian G Leroux, Xingye Lei, and Norman Breslow. Estimation of disease rates in small areas: a new mixed model for spatial dependence. In *Statistical models in epidemiology, the environment, and clinical trials*, pages 179–191. Springer, 2000.
- Ying C MacNab. Bayesian disease mapping: Past, present, and future. *Spatial Statistics*, 50:100593, 2022.
- Thiago G Martins, Daniel Simpson, Finn Lindgren, and Håvard Rue. Bayesian computing with inla: new features. *Computational Statistics & Data Analysis*, 67: 68–83, 2013.
- Swapnil Mishra, Seth Flaxman, Tresnia Berah, Mikko Pakkanen, Harrison Zhu, and Samir Bhatt. *pi vae*: Encoding stochastic process priors with variational autoencoders. *Statistics & Computing*, 2022.

- Du Phan, Neeraj Pradhan, and Martin Jankowiak. Composable effects for flexible and accelerated probabilistic programming in numpyro. *arXiv preprint arXiv:1912.11554*, 2019.
- Heidi Reid, Ubydul Haque, Archie CA Clements, Andrew J Tatem, Andrew Vallely, Syed Masud Ahmed, Akramul Islam, and Rashidul Haque. Mapping malaria risk in bangladesh using bayesian geostatistical models. *The American journal of tropical medicine and hygiene*, 83(4):861, 2010.
- Andrea Riebler, Sigrunn H Sørbye, Daniel Simpson, and Håvard Rue. An intuitive bayesian spatial model for disease mapping that accounts for scaling. *Statistical methods in medical research*, 25(4):1145–1165, 2016.
- Christian P Robert, George Casella, and George Casella. *Monte Carlo statistical methods*, volume 2. Springer, 1999.
- Elizaveta Semenova, Yidan Xu, Adam Howes, Theo Rashid, Samir Bhatt, Swapnil Mishra, and Seth Flaxman. Priorvae: encoding spatial priors with variational autoencoders for small-area estimation. *Journal of the Royal Society Interface*, 19(191):20220094, 2022.
- Elizaveta Semenova, Max Cairney-Leeming, and Seth Flaxman. PriorCVAE: scalable MCMC parameter inference with Bayesian deep generative modelling. *arXiv preprint arXiv:2304.04307*, 2023.
- Robert W Snow, Benn Sartorius, David Kyalo, Joseph Maina, Punam Amratia, Clara W Mundia, Philip Bejon, and Abdisalan M Noor. The prevalence of plasmodium falciparum in sub-saharan africa since 1900. *Nature*, 550(7677):515–518, 2017.
- Yusuke Tanaka, Toshiyuki Tanaka, Tomoharu Iwata, Takeshi Kurashima, Maya Okawa, Yasunori Akagi, and Hiroyuki Toda. Spatially aggregated gaussian processes with multivariate areal outputs. *Advances in Neural Information Processing Systems*, 32, 2019.
- U.S. President’s Malaria Initiative. U.s. president’s malaria initiative kenya malaria operational plan fy 2022. retrieved from www.pmi.gov. 2022.
- Aki Vehtari, Andrew Gelman, Daniel Simpson, Bob Carpenter, and Paul-Christian Bürkner. Rank-normalization, folding, and localization: an improved r for assessing convergence of mcmc (with discussion). *Bayesian analysis*, 16(2):667–718, 2021.
- Jonathan C Wakefield, NG Best, and L Waller. Bayesian approaches to disease mapping. *Spatial epidemiology: methods and applications*, 59, 2000.
- Daniel J Weiss, Tim CD Lucas, Michele Nguyen, Anita K Nandi, Donal Bisanzio, Katherine E Battle, Ewan Cameron, Katherine A Twohig, Daniel A Pfeffer, Jennifer A Rozier, et al. Mapping the global prevalence, incidence, and mortality of plasmodium falciparum, 2000–17: a spatial and temporal modelling study. *The Lancet*, 394(10195):322–331, 2019.
- Fariba Yousefi, Michael T Smith, and Mauricio Alvarez. Multi-task learning for aggregated data using gaussian processes. *Advances in Neural Information Processing Systems*, 32, 2019.
- Harrison Zhu, Adam Howes, Owen van Eer, Maxime Rischard, Yingzhen Li, Dino Sejdinovic, and Seth Flaxman. Aggregated gaussian processes with multiresolution earth observation covariates. *arXiv preprint arXiv:2105.01460*, 2021.